A Unified Gas and Power Flow Analysis in Natural Gas and Electricity Coupled Networks

Alberto Martínez-Mares and Claudio R. Fuerte-Esquivel, *Senior Member, IEEE*

***Abstract*—The restructuring of energy markets has increased the concern about the existing interdependency between the primary energy supply and electricity networks, which are analyzed traditionally as independent systems. The aim of this paper is focused on an integrated formulation for the steady-state analysis of electricity and natural gas coupled systems considering the effect of temperature in the natural gas system operation and a distributed slack node technique in the electricity network. A general approach is described to execute a single gas and power flow analysis in a unified framework based on the Newton–Raphson formulation. The applicability of the proposed approach is demonstrated by analyzing the Belgian gas network combined with the IEEE-14 test system and a 15-node natural gas network integrated with the IEEE-118 test system.**

***Index Terms*—Electricity infrastructure, natural gas infrastructure, Newton method, power flow analysis.**

NOMENCLATURE

A. Indices

i, j	Index of electrical system nodes.
k, m	Index of natural gas system nodes.
N_e	Nodes in the electrical system.
N_{PV}	PV-type nodes in the electrical system.
N_{ng}	Nodes in the natural gas system.
N_p^k	Number of pipelines connected at kth node.
N_C	Number of compressors in the natural gas system.

B. Constants

g	32.2178 gravitational constant (ft/s^2).
GHV	1015, gross heating value (BTU/SCF).
R_G	10.7316 gas constant (PSI ft^3/lbmol°R).
MW_{air}	28.96, air molecular weight.

C. Parameters

ρ_k	Gas-specific heat ratio (dimensionless).
C_p	Gas heat capacity at constant pressure (dimensionless).
D^{km}	Inner diameter of pipe linking nodes km (in).
E_C	Compressor's parasitic efficiency (dimensionless).
E_p	Pipeline's efficiency (dimensionless).
H_k	Pipeline's inlet elevation (ft).
H_m	Pipeline's outlet elevation (ft).
L^{km}	Pipeline's length from node k to node m (miles).
$\prod_b$	Pressure base (PSIA).
R^{km}	Compression ratio (dimensionless).
T_b	Base temperature (°R).
U^{km}	Heat transfer coefficient at pipe from k to m (BTU/ft^2)
Z_a	Supercompressibility factor (dimensionless).
η_c	Compression process efficiency (dimensionless).
α_C^{km}, β_C^{km} and γ_C^{km}	Compressors gas consumption coefficients.
α_g^i, β_g^i, and γ_g^i	Heat rate coefficients for coupled nodes.
η_{JT}	Joule-Thompson coefficient (°R/PSIA).
γ_G	Gas specific gravity (dimensionless).
G_{ij}	Conductance of the nodal admittance matrix (p.u.).
B_{ij}	Susceptance of the nodal admittance matrix (p.u.).

Manuscript received September 19, 2011; revised January 17, 2012; accepted March 13, 2012. Date of publication May 04, 2012; date of current version October 17, 2012. This work was supported by CONACyT, México under Grant 94349 and Research Project 106198. Paper no. TPWRS-00892-2011.

The authors are with the Electrical Engineering Faculty, Universidad Michoacana de San Nicolás de Hidalgo (UMSNH), Morelia, Michoacan, 58000, Mexico (e-mail: amartinez@faraday.fie.umich.mx; cfuerte@umich.mx).

Digital Object Identifier 10.1109/TPWRS.2012.2191984

D. Variables

BHP^{km}	Energy consumption for the compression station connecting nodes km (HP).
f	Darcy–Weisbach friction factor (dimensionless).
ΔM	Vector of natural gas nodal balance.
ΔHP	Vector of compressors energy consumption.
ΔR	Vector of compression ratio functions.
ΔT_g	Vector of thermal equilibrium functions.
H_p^{km}	Slope pipeline correction from k to m (PSIA^2).
m_G	Mass of natural gas (lb_m/s).
T_a^{km}	Gas average temperature for the pipeline connecting nodes km (°R).
T_k	Final temperature of a mixture of several natural gas injections (°R) at kth node.
T_m^{km}	Gas temperature at node mth in the natural gas flowing from k to m (°R).
T_s^{km}	Average temperature of the environment surrounding the pipeline connecting nodes km (°R).
P_{gen}^i	Generation of active power at ith (p.u.).
Q_{gen}^i	Generation of reactive power at ith node (p.u.).
P_{gen}^{i0}	Set-point of active power generation at ith node (p.u.).
ΔP_{gen}	Additional active power supplied by slack nodes (p.u.).
k_{gen}^i	Participation factor of the i generation (dimensionless).
P_{load}^i	Demand of active power at ith node (p.u.)
Q_{load}^i	Demand of reactive power at ith node (p.u.).
P_{cal}^i	Calculated active power injected at ith node (p.u.).
Q_{cal}^i	Calculated reactive power injected at ith node (p.u.).
$L_{\mathrm{comp}}^{km,i}$	Active power demanded by the compressor motors (p.u.).
$M_{gl}^{k,i}$	Gas load driven the ith electric generator (SCFD).
M_p^{km}	Pipeline's natural gas flow (SCFD).
M_C^{km}	Compressor natural gas flow (SCFD).
M_{gl}^k	Natural gas load at kth node (SCFD).
M_{gs}^k	Natural gas injection at kth node (SCFD).
M_{total}^k	Total natural gas injected by pipelines and compressors at kth node (SCFD).
$\lvert V_i\rvert$	Voltage magnitude at ith node (p.u.).
x_{ng}	State variables for the natural gas system.
x_e	State variables for the electric power system.
X	State variables for the coupled systems.
$\prod_a^{km}$	Average pressure for the pipeline connecting nodes k and m (PSIA).
$\prod_k$	Pressure at the kth node (PSIA).
τ_C^{km}	Gas extracted from the kth node by the compressor connecting nodes k and m (SCFD).
δ_i	Voltage angle at ith node (rad).
ρ_G^{km}	Gas density calculated for the pipeline connecting nodes k and m (lbm/ft^3).

I. Introduction

THE secure and reliable operation of an electric power system depends not only on the availability and performance of the electric generation and transmission facilities but also on its interdependency with those infrastructures used to produce, transport, and store the various forms of primary energy that are transformed into electricity. Traditionally, all of these infrastructures have been designed and operated separately from each other; however, the restructuring of energy systems in several parts of the world has increased the interest in evaluating in a coordinated manner the interdependency existing between the individual primary energy and electricity sectors in order to determine how the state of each infrastructure affects the economic and secure operation of the overall energy grid. Among all types of primary energy systems, electric power generation relies increasingly on the natural gas supply system as additional natural gas-fired power plants are installed in power systems because of their low cost and environmental impact [1], such that electric power and natural gas systems are becoming increasingly interdependent.

There are several proposals for modeling the combined natural gas and electricity infrastructures by a single integrated formulation to achieve an optimal operation of the coupled energy

system. In [2], the interdependency of both structures is evaluated in terms of the impact of the gas market prices on the unit commitment and dispatch. Hence, the gas infrastructure is not modeled directly, and the interdependency is only considered through the production cost of natural gas-fired plants given by the gas market price times their gas consumption. In [3], both infrastructures are represented as networks composed of nodes and arcs that possess capacity and efficiency constraints. The economic efficiencies of the energy flows in the integrated energy system are then evaluated. Appropriately chosen multipliers on the arcs represent energy losses, such that the technical operating parameters of the infrastructures are omitted in the model.

Other proposals concerned with optimal power flow studies in combined natural gas and electricity networks explicitly take into account the former infrastructure [4][5][6][7][8]. These proposals consider equality constraints associated with the balance of the injected power and injected gas, which must be satisfied at each node in the electrical and natural gas systems, respectively, considering the nodal voltages and nodal pressures as state variables. The static security constraints associated with the operation of both infrastructures are related to nodal voltage magnitudes, thermal limits in transmission lines, generation limits of active and reactive powers, nodal pressures and compression rates, as well as the injection and consumption of gas. Other constraints have also been considered: the maximum flow rate in natural gas pipes [5], natural gas contracts and reserves [7] and the linepack of a pipeline [8]. In [6], the coupling of both infrastructures is explicitly studied via an energy hub that represents the energy interaction through coupling matrices whose elements correspond to efficiency and conversion factors; no other quantities are used. The maximum amount of energy that can be provided from the natural gas system to each gas-fired electric generator is computed in [5] by modeling these generators as natural gas loads; thus, the electric transmission network is not considered in the study. On the other hand, the electricity network is represented by a direct current model in [7] and [8].

Several assumptions are adopted in all above-mentioned references to simplify the gas flow calculations by using Weymouth's formula, which neglects changes in the altitude over the pipeline, in the compressibility factor, and in gas temperature along the pipeline among others [9], [10]. However, the gas temperature must be determined in combination with nodal pressure profiles to define suitable operational conditions that avoid the hydrate formation in the inner-wall of a pipeline, natural gas fluctuations, the excessive energy consumption in compression stations and the condensation of gas [10], [11], as well as assuring the quality of the natural gas supplied at each gas-fired generator in order to maximize the efficiency in the energy conversion cycle [12]. Hence, the gas temperature must be considered as a variable in the gas flow equation.

In the context of electricity infrastructures, their daily operation relies on extensive power flow studies to indicate whether or not the nodal voltage magnitudes and power flows in transmission components are within prescribed operating limits. However, the power flow solution is obtained without considering both the availability of primary energy supply and the primary energy network operating condition, i.e., the natural gas infrastructure. Hence, apart from optimal power flow studies, a crucial study to quantify the interdependency of energy infrastructures is related to the computation of an equilibrium point by using an energy flow algorithm, whose results will provide the initial operating condition to perform higher hierarchy level of power system studies. Therefore, in order to address the challenge of analyzing the steady-state interdependency between natural gas and electricity networks and considering that the power flow analysis is the cornerstone of power system studies, this paper proposes a unified approach for the solution of the gas and power flow problem in both infrastructures for a time horizon corresponding to a single time period (snapshot). This problem is formulated individually for each system based on the balance of nodal flows, representing the gas flow equations of the natural gas system in a consistent manner with regards to their counterparts in the electrical system, and a generic framework is then proposed to execute the flow analysis in conjunction for both systems. In this context, the gas temperature is viewed as a variable in the gas flow equation based on the proposal detailed in [13] in order to identify operating conditions with risk of hydrate formation and to assess its effect on the energy consumed by compressors. On the other hand, the conventional electric power flow formulation assumes the existence of a slack generator that supplies the entire imbalance of active power in the system, even when a sufficient spinning reserve exists on other generators. However, as pointed out in [14], "a slack bus is something artificial which has no relation to the physical system since no such distinction exists among generators." In order to overcome this shortcoming, the concept of distributed slack nodes is used in the proposed approach; thus, the active power output of an arbitrary number of generators is adjusted to achieve a total active power balance in the electric power system. The use of this concept justifies the unified model proposed to assess the equilibrium point of the overall energy grid. In addition, it also increases the value of the proposed approach because the adjustments of active power generation as a function of the gas supply and the electric energy consumed by compressor motors are computed during the solution process in a closed loop computation, more realistically representing the interdependency between both infrastructures.

Finally, the set of nonlinear algebraic equations representing both systems is solved by using Newton's method in order to assess the values of state variables that provide the steady-state of the overall energy grid under a prespecified operating condition.

The proposed approach is described in detail in the remainder of this paper as follows. Section II presents a detailed gas flow and thermal balance formulation for the natural gas infrastructure considering pipelines and compressor elements, Section III describes the electric power system modeling for steady-state analysis considering distributed slack nodes and Section IV presents the formulation to integrate both systems and the unified solution of the whole set of nonlinear equations by Newton's approach. The application of the proposed approach to two coupled energy systems is presented in Section V. Finally, Section VI presents the conclusions of this work.

II. Natural Gas System Formulation

The steady-state modeling of a natural gas system is formulated by the equations related to the gas flow and to the thermal behavior of the gas in those elements composing the system. The gas flow balance is also formulated to assess the equilibrium point condition at each system's node. For the purpose of this paper, the elements considered are pipelines, compressors, sources, and loads. The storage elements are modeled as sources or as loads depending on their operating condition.

A. Pipeline Equation

Several equations have been proposed to compute the gas flow through pipelines [11], the main difference between them being how the friction coefficient term and natural gas characteristics are considered in the formulation. In this context, the following equation is the most commonly used to compute the gas flow in a pipeline between gas nodes k and m [10], [15] and is the one employed in this paper:

$$M_p^{km} = \mathrm{sgn}_p\left(\Pi_k, \Pi_m, H_p^{km}\right)\left(\frac{77.54T_b}{\Pi_b}\right)D^{2.5} \times \left(\frac{\left|\Pi_k^2 - \Pi_m^2 - H_p^{km}\right|}{L^{km}\gamma_G T_a^{km} Z_a f}\right)^{0.5} E_p \quad (1)$$

where $\mathrm{sgn}_p(\Pi_k, \Pi_m, H_p^{km}) = 1$ if $(\Pi_k^2 - \Pi_m^2 - H_p^{km}) > 0$ or $\mathrm{sgn}_p(\Pi_k, \Pi_m, H_p^{km}) = -1$ if $(\Pi_k^2 - \Pi_m^2 - H_p^{km}) < 0$.

Note from (1) that higher natural gas flows with lower pressure drops occur in those pipelines which are colder, shorter, and more efficient [15].

Based on the knowledge of the network and the experience of engineers that operate the gas infrastructure, the physical characteristics of each pipeline and the gas composition in (1) can be expressed by a single constant C_{km} given by

$$C_{km} = \left(\frac{77.54T_b}{\Pi_b}\right)D^{2.5}\left(\frac{1}{L^{km}\gamma_G T_a^{km} Z_a f}\right)^{0.5} E_p. \quad (2)$$

The term H_c^{km} considers the effect of changes in the altitude over the pipeline and is calculated by

$$H_p^{km} = \frac{0.0375g(H_m - H_k)\left(\Pi_a^{km}\right)^2}{Z_a T_a^{km}} \quad (3)$$

where the average pressure Π_a^{km} is calculated by (4), which considers the nonlinear pressure drop with distance [15]

$$\Pi_a^{km} = \frac{2}{3}\left[(\Pi_k + \Pi_m) - \left(\frac{\Pi_k \Pi_m}{\Pi_k + \Pi_m}\right)\right]. \quad (4)$$

The average temperature T_a^{km} used in (2) and (3) is computed considering the nonlinear effect of distance and the weather to which pipelines are exposed [10]

$$T_a^{km} = T_s^{km} + \frac{T_k - T_m}{\ln\left(\frac{T_k - T_s^{km}}{T_m - T_s^{km}}\right)}. \quad (5)$$

The friction factor value strictly depends on the inner diameter of the pipeline for high pressure networks working in the fully turbulent flow region [4] and is given by

$$f = \frac{0.032}{D^{\frac{1}{3}}}. \quad (6)$$

B. Compression Station Equations

Compression stations are installed in gas pipelines to compensate for the loss of pressure due to both the friction of pipes and the heat transfer between the gas and its environment, as well as to provide the pressure needed to transport gas from one location to another [10]. A compression station connected between nodes k and m is mathematically represented, respectively, by its energy consumption and by its compression ratio as follows:[4]

$$BHP^{km} = 0.0854 Z_a\left[\frac{M_C^{km} T_k}{E_C \eta_C}\right]\left[\frac{c_k}{c_k - 1}\right]\left[\left(\frac{\Pi_m}{\Pi_k}\right)^{\frac{c_k - 1}{c_k}} - 1\right] \quad (7)$$

$$\Pi_k R^{km} = \Pi_m. \quad (8)$$

The energy required by the compressor to increase the pressure level can be provided by an electric motor or a gas-fired turbine; in the former, the energy could be supplied from the ith node of the electric power system and is calculated by

$$L_{\mathrm{comp}}^{km,i} = BHP^{km}\left(\frac{0.000007457}{3600}\right) \quad (9)$$

while the gas required for the gas-fired turbine is extracted from the natural gas network as given by

$$\tau_C^{km} = \alpha_C^{km} + \beta_C^{km} BHP^{km} + \gamma_C^{km}\left(BHP^{km}\right)^2. \quad (10)$$

C. Nodal Gas Balance Equation

A nodal gas flow balance must be satisfied at each node of the gas infrastructure to assure that the sum of the gas entering and injected is equal to the sum of the gas leaving the node and the total gas withdrawal, as given by

$$\Delta M_k = \sum_{m\in k} M_p^{km} + \sum_{m\in k} \mathrm{sgn}_c(k,m) M_C^{km} + \sum_{m\in k} \tau_C^{km} - M_{gs}^k + M_{gl}^k = 0 \quad \forall k = 1, \cdots, (N_{ng} - 1) \quad (11)$$

where $\Sigma_{m\in k}$ is the set of nodes adjacent to node k, $\mathrm{sgn}_c(k,m) = 1$ if the compressor unit has its inlet at node k; otherwise, $\mathrm{sgn}(k,m) = -1$.

Note that at least one nodal pressure must be specified in order to perform the gas flow analysis. A known-nodal pressure is taken as a reference to compute all other unknown nodal pressures, and the gas injection computed at this node will provide the gas flow balance in the network by compensating for the gas consumed by compressors. In this case, the corresponding gas balance equation associated with this slack node is not included in the mathematical formulation, but is solved separately by finding the gas injected at this node once the steady-state of the overall energy grid has been computed.

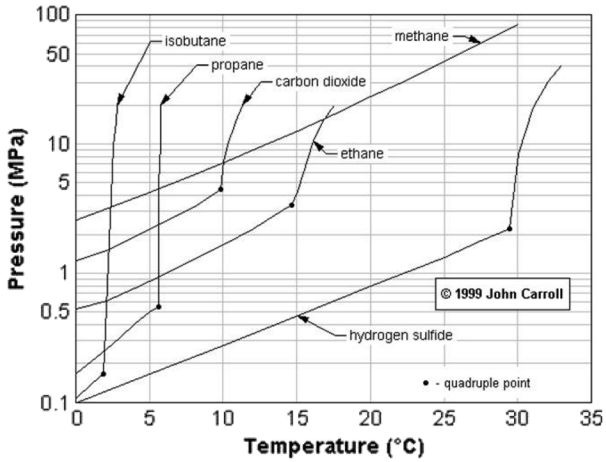

Fig. 1. Hydrate formation chart [16].

D. Thermal Formulation

The knowledge of gas temperature at each node of the network permits the definition of the heaters' location to prevent hydrate formation or gas condensation, the gas inlet temperature for compressors, and the minimum gas flow values in the network [10]. The hydrates could originate critical operating problems, because they could be deposited in the inner wall of a pipeline and block the gas flow. The solution of this problem represents great technical difficulties and high maintenance costs [10], [16].

Several methods to evaluate formations of hydrates have been reported in the literature [10], one of the most used approaches being the chart proposed in [16] and shown in Fig. 1. Natural gas is composed mainly of methane, and, as reported in this chart, higher operation pressures require higher gas temperature conditions in order to keep the gas composition in a safety zone (the right-hand side of the curve) to avoid formation of hydrates. By way of example, the risk of hydrate formation increases for gas temperatures below 14 °C considering an operation pressure of 10 MPa.

The temperature at node k of gas flowing in a pipeline connecting nodes k and m is computed by

$$T_k^{km} = \left\{ T_k - \left[T_s^{km} + \left(\frac{\eta_{JT}}{a}\right)\left(\frac{\Pi_k - \Pi_m}{L^{km}}\right)\right]\right\} e^{-aL^{km}} + \left[T_s^{km} + \left(\frac{\eta_{JT}}{a}\right)\left(\frac{\Pi_k - \Pi_m}{L^{km}}\right)\right] \quad (12)$$

based on the proposal detailed in [13], which considers that the gas temperature starts at the inlet pipe's temperature and tends to the surrounding pipe's temperature as the gas flows through the pipeline, where

$$a = \frac{\pi D^{km} U^{km}}{m_G C_P} \quad (13)$$

$$m_G = Q_p^{km}\left(\frac{\Pi_b}{\Pi_k}\right)\left(\frac{T_k}{T_b}\right) Z_a \left(\frac{1}{86400}\right)\rho_G^{km} \quad (14)$$

$$\rho_G^{km} = \frac{\Pi_k \gamma_G M W_{\text{air}}}{Z_a R_G T_k}. \quad (15)$$

When gas injections with different temperatures arrive to a given node from different pipelines and compressors, a calculation of the thermal equilibrium of the nodal gas mixture based on the heat transfer theory is necessary [17]. Therefore, the thermal equilibrium at the kth node is given by

$$T_k = \sum_{m\in k} \frac{M_p^{mk}}{M_{\text{total}}^k} T_k^{mk} + \sum_{j\in k} \frac{M_c^{jk}}{M_{\text{total}}^k} T_k^{jk}, \quad \forall k = 1, \cdots, N_{ng} \quad (16)$$

where $\Sigma_{m\in k}(\Sigma_{j\in k})$ is the set of nodes adjacent to node k from which the gas is flowing into node k through a pipeline (compressor). In this case, the same temperature value at both ends of the compression stations is assumed.

E. Natural Gas State Variables

Equations (7), (8), (11), and (16) are used to assess the equilibrium point of the natural gas network by computing the values of nodal pressures, nodal temperatures, as well as energy consumption and gas flowing in compressors, $[x_{ng}] = [\Pi, T, BHP, M_C]^{\text{t}}$, for given values of nodal pressures in known-pressure nodes and of nodal gas injections in all other nodes that do not supply energy to gas-fired power plants. In this formulation, $\Pi \in \Re^{(N_g-1)}$, $T \in \Re^{N_g}$, $BHP \in \Re^{N_C}$, and $M_C \in \Re^{N_C}$, respectively.

III. Electricity System Formulation

An ac power flow model is used to represent the electricity network, which is already well documented in [18]. The steady-state operation of a power system is formulated by stipulating that, at each system's node, the power injected by generators, the power demanded by loads, and powers exchanged through the transmission elements connected to the node must add up to zero. This applies to both active and reactive powers. These equations are termed mismatch power equations and take the following form at node i [18]:

$$\Delta P_i = P_{\text{gen}}^i - P_{\text{load}}^i - P_{\text{cal}}^i = 0 \qquad \forall i = 1, \cdots, N_e \quad (17)$$

$$\Delta Q_i = Q_{\text{gen}}^i - Q_{\text{load}}^i - Q_{\text{cal}}^i = 0, \quad \forall i = 1, \cdots, (N_e - N_{PV}) \quad (18)$$

where

$$P_{\text{cal}}^i = \sum_{j\in i} \{ V_i^2 G_{ii} + V_i V_j [G_{ij}\cos(\theta_i - \theta_j) + B_{ij}\sin(\theta_i - \theta_j)]\} \quad (19)$$

$$Q_{\text{cal}}^i = \sum_{j\in i} \{ -V_i^2 B_{ii} + V_i V_j [G_{ij}\sin(\theta_i - \theta_j) - B_{ij}\cos(\theta_i - \theta_j)]\}. \quad (20)$$

The equilibrium point of the power system is obtained by solving the set of (17) and (18) for the voltage magnitudes and phase angles at all nodes in the network $[x_e] = [V, \theta]$ by knowing the generations and loads in the system. The active and reactive power flows throughout the transmission system are then determined according to (19) and (20). Since the power transmission losses cannot be calculated without knowing the power flow through the transmission elements, one of the generator nodes is designated to pick up this slack in power generation, which is referred to as slack node, with its voltage magnitude and phase angle assumed to be known. The latter is

chosen as the reference against which all other voltage phase angles in the system are measured.

In order to overcome the shortcoming of only adjusting the active power of a single slack generator to achieve a total active power balance, the concept of distributed slack nodes is used in this paper [14]. In this case, the active power output of a selected number of generators is regulated during the power flow solution, based on their assigned participation factors, to supply the generation required to satisfy the entire active power imbalance in the system. Hence, the variable active power of regulating generators is defined as

$$P^i_{\text{gen}} = P^{i0}_{\text{gen}} + k^i_{\text{gen}} \Delta P_{\text{gen}} \qquad \forall i \in N_e \tag{21}$$

$$\sum_{i \in N_{rg}} k^i_{\text{gen}} = 1 \tag{22}$$

where ΔP_{gen} is the unknown additional generation of active power required to satisfy the existing imbalance between the set-point system generation and the total active power demand plus transmission losses.

In this approach, the slack node is considered to be like any of the other system's nodes, with corresponding active and reactive power mismatch equations, and the reference voltage phase angle can be arbitrarily selected at any of the system nodes. In addition to the standard classification of system nodes into generator voltage-controlled (PV), generator voltage-uncontrolled (PQ) and load (PQ) nodes [18], two new node types are defined: a generator PV node with variable active power generation and a generator PQ node with variable active power generation. In these nodes, the active power output constraints imposed on regulating gas-fired generators correspond to the generators' own operational limits and to the amount of natural gas that can be extracted from the gas network. If any regulating generator reaches one of its active power generation limits, its active power output is fixed at the offended limit for the remaining of the power flow solution process, and the active power balance of the system is provided by the rest of regulating generators. On the other hand, even though the reactive power mismatch (18) of a PV node is not considered in the formulation, it is solved at each iterative step to assess whether or not the generator reactive power is within limits. If the generator cannot provide the necessary reactive power support to constrain the voltage magnitude at the specified value then the reactive power is fixed at the violated limit and the voltage magnitude is freed. Finally, the unknown vector of state variables that determine the power system's equilibrium point is now given by $[x_e] = [V, \theta, \Delta P_g]$, where $V \in \Re^{(N_e - N_{PV})}$, $\theta \in \Re^{(N_e - 1)}$, and $\Delta P_{\text{gen}} \in \Re$.

IV. Combined Natural Gas and Electric Power Flow Formulation

A. Heat Rate Curve

The relationship between the natural gas and electricity networks is provided by the gas-fired turbines' generators, which act as energy converters. This coupling is mathematically formulated by

$$HR^i = \alpha^i_g + \beta^i_g P^i_{gen} + \gamma^i_g \left(P^i_{gen}\right)^2 \tag{23}$$

referred to as the heat rate curve, which represents the efficiency conversion of the energy contained in natural gas at the kth node into electrical energy injected at the ith node of the electrical network

Additionally, the gas flow required for the energy demanded by the heat rate curve is computed by

$$M^{k,i}_{gl} = \frac{HR^i}{GHV}. \tag{24}$$

Note that the gas consumed by a gas-fired turbine is a function of the active power generated by the unit and the natural gas available at the extraction node.

B. Unified Gas and Power Flow Solution

The integrated gas and power flow formulation of the natural gas and electricity infrastructures is obtained by combining the stated flow models considering the link between both infrastructures through gas-fired power plants connected to gas pipelines and compressors using electrical energy. Hence, the set of nonlinear equations that has to be solved for the state variables of both infrastructures is given by

$$\begin{aligned}\Delta M_k = &\sum_{m \in k} M^{km}_p + \sum_{m \in k} \text{sgn}_c(k,m) M^{km}_C + \sum_{m \in k} \tau^{km}_C \\ &- M^k_{gs} + M^k_{gl} + M^{k,i}_{gl} = 0 \\ &\forall k = 1, \cdots, (N_{ng} - 1)\end{aligned} \tag{25}$$

$$\begin{aligned}\Delta T_k = &T_k - \sum_{m \in k} \frac{M^{mk}_p}{M^k_{\text{total}}} T^{mk}_k \\ &+ \sum_{j \in k} \frac{M^{jk}_c}{M^k_{\text{total}}} T^{jk}_k = 0 \qquad \forall k = 1, \cdots, N_{ng}\end{aligned} \tag{26}$$

$$\begin{aligned}\Delta HP^{km}_C = &BHP^{km} - 0.0854 Z_a \left[\frac{M^{km}_C T_k}{E_C \eta_C}\right] \left[\frac{c_k}{c_k - 1}\right] \\ &\left[\left(\frac{\Pi_m}{\Pi_k}\right)^{\frac{c_k - 1}{c_k}} - 1\right] \quad \forall C \in N_C, \quad k \in N_{ng}, \\ &m \in N_{ng}, \quad k \neq m\end{aligned} \tag{27}$$

$$\begin{aligned}\Delta R^{km}_C = &\frac{\Pi_m}{\Pi_k} - R^{km} = 0 \quad \forall C \in N_C, \quad k \in N_{ng}, \\ &m \in N_{ng}, \quad k \neq m.\end{aligned} \tag{28}$$

$$\begin{aligned}\Delta P_i = &\left(P^{i0}_{\text{gen}} + k^i_{\text{gen}} \Delta P_{\text{gen}}\right) - P^i_{\text{load}} - P^i_{\text{cal}} - L^{km,i}_{\text{comp}} = 0 \\ &\forall i = 1, \cdots, N_e\end{aligned} \tag{29}$$

$$\begin{aligned}\Delta Q_i = &Q^i_{\text{gen}} - Q^i_{\text{load}} - Q^i_{\text{cal}} = 0, \\ &\forall i = 1, \cdots, (N_e - N_{PV}).\end{aligned} \tag{30}$$

The proposed unified solution approach consists of applying Newton's method to provide an approximate solution to the total set of equality constraints $F(X) = [\Delta M, \Delta T_g, \Delta HP, \Delta R, \Delta P, \Delta Q,]^t = 0$, where $\Delta M \in \Re^{(N_{ng}-1)}$, $\Delta T_g \in \Re^{N_{ng}}$, $\Delta HP \in \Re^{N_C}$, $\Delta R \in \Re^{N_C}$, $\Delta P \in \Re^{N_e}$, and $\Delta Q \in \Re^{(N_e - N_{PV})}$, by solving for $\Delta X = [\Delta x_{ng}, \Delta x_e]^t$ in the linear problem $J^\ell \Delta X^\ell = -F(X^\ell)$, where J is known as the Jacobian matrix and is given in expanded form by (31), shown at the bottom of the next page. For given initial values of $X^\ell = [x^\ell_{ng}, x^\ell_e]^{\text{t}}$, the method updates the

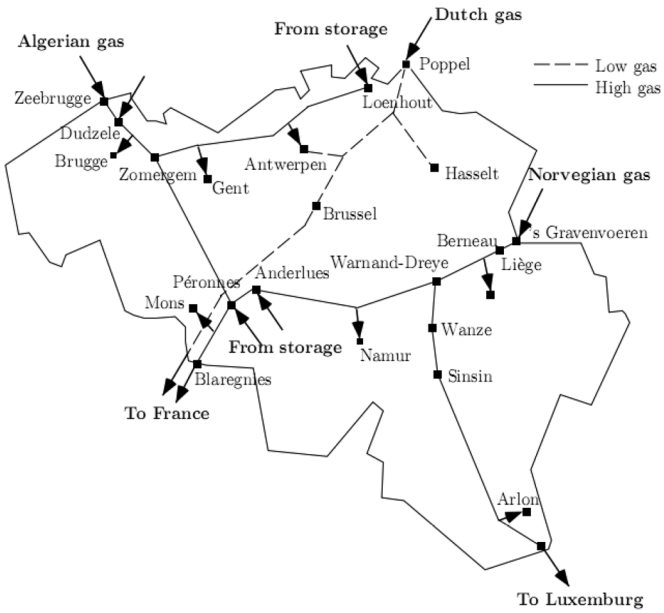

Fig. 2. Belgium natural gas transmission system [20].

solution, $[x_{ng}^{\ell+1} = x_{ng}^{\ell} + \Delta x_{ng}^{\ell}, x_{e}^{\ell+1} = x_{e}^{\ell} + \Delta x_{e}^{\ell}]^{\mathrm{t}}$, at each iteration ℓ until $F(X^{\ell})$ satisfies a predefined tolerance. The need to efficiently solve the large set of sparse linearized equations $J^{\ell}\Delta X^{\ell} = -F(X^{\ell})$ requires the use of sparsity techniques, where the ordering for sparsity factorization of the Jacobian matrix is carried out according to the Tinney-2 scheme [19].

C. Initialization

The attractiveness of using Newton's method is that it arrives at the solution with local quadratic convergence regardless of the network size if all state variables involved in the study are suitably initialized and the Jacobian matrix is nonsingular at the solution point [20].

For the electric power system, the voltage magnitudes are initialized at 1 p.u. at all uncontrolled voltage magnitude nodes, while the controlled PV nodes are initialized at specified values that remain constant throughout the iterative solution if no generator reactive power limits are violated. The initial voltage phase angles are selected to be 0 at all buses [21]. The unknown additional generation of active power ΔP_{gen} is initialized in zero.

In contrast to the electric power systems, special caution should be taken to initialize the state variables of the gas infrastructure. By way of example, the gas flow through the gas infrastructure is a function of the difference of pressures at the pipeline's ends such that initialization of pressures gives rise to an ill-conditioned Jacobian matrix if a flat initialization is adopted when changes in the pipeline's altitude are not taken into account. In such a situation, the linearized mass flow equation yields a null diagonal element in the Jacobian.

The strategy adopted to remedy this situation consists of selecting the initial values for nodal pressures at the pipeline's ends considering a difference of pressures of $5 \sim 10\%$ between the receiving and sending nodes, taking as a reference value the specified pressure at the slack node. This initialization process is adopted independently of how the changes in the pipeline's altitude are being considered.

Since the gas temperature tends to the environmental temperature surrounding each pipeline, the nodal temperatures are initialized at the value T_s^{km}. The gas flowing in all compressors is initialized at the same value given by the average value

TABLE I
NATURAL GAS FLOWS AT PIPELINES

Pipeline	C_{km} (SCF/PSIA)	From	To	Gas flow (SCF^3/hour) 1.a)	1.b)	1.c)	1.d)
1	6566436	1	2	10.80	10.81	10.80	10.81
2	6566436	1	2	10.80	10.81	10.80	10.81
3	4912482	2	3	15.62	15.62	15.62	15.62
4	4912482	2	3	15.62	15.62	15.62	15.62
5	4326324	3	4	25.47	25.49	25.47	25.49
6	240319	5	6	0.562	0.561	0.562	0.562
7	1175149	6	7	-5.373	-5.373	-5.373	-5.373
8	764054	7	4	-13.10	-13.10	-13.10	-13.10
9	1728699	4	14	11.67	11.67	11.67	11.67
10	1144991	8	9	26.76	26.76	26.76	26.76
11	123179	8	9	2.879	2.879	2.879	2.879
12	4907626	9	10	19.75	19.75	19.75	19.75
13	2457651	9	10	9.892	9.892	9.892	9.892
14	3641178	10	11	12.45	12.45	12.45	12.45
15	2285681	10	11	7.820	7.820	7.820	7.820
16	2869666	11	12	17.75	17.75	17.75	17.75
17	3497039	12	13	14.028	14.02	14.02	14.02
18	5874893	13	14	19.31	19.30	19.31	19.30
19	3500118	14	15	33.05	33.05	33.05	33.05
20	2491576	15	16	22.97	22.97	22.97	22.97
21	109941	11	17	2.522	2.522	2.522	2.522
22	160430	17	18	2.522	2.522	2.522	2.522
23	304984	18	19	2.522	2.522	2.522	2.522
24	204329	19	20	2.823	2.823	2.823	2.823

$$J = \left[\begin{array}{cccc|ccc} \frac{\partial \Delta M}{\partial \Pi} & \frac{\partial \Delta M}{\partial T} & \frac{\partial \Delta M}{\partial BHP} & \frac{\partial \Delta M}{\partial M_C} & 0 & 0 & \frac{\partial \Delta M}{\partial \Delta P_{\mathrm{gen}}} \\ \frac{\partial \Delta T_g}{\partial \Pi} & \frac{\partial \Delta T_g}{\partial T} & 0 & \frac{\partial \Delta T_g}{\partial M_C} & 0 & 0 & 0 \\ \frac{\partial \Delta HP}{\partial \Pi} & \frac{\partial \Delta HP}{\partial T} & \frac{\partial \Delta HP}{\partial BHP} & \frac{\partial \Delta HP}{\partial M_C} & 0 & 0 & 0 \\ \frac{\partial \Delta R}{\partial \Pi} & 0 & 0 & 0 & 0 & 0 & 0 \\ \hline 0 & 0 & \frac{\partial \Delta P}{\partial BHP} & 0 & \frac{\partial \Delta P}{\partial \theta} & \frac{\partial \Delta P}{\partial V} & \frac{\partial \Delta P}{\partial \Delta P_{\mathrm{gen}}} \\ 0 & 0 & 0 & 0 & \frac{\partial \Delta Q}{\partial \theta} & \frac{\partial \Delta Q}{\partial V} & 0 \end{array}\right] \tag{31}$$

TABLE II
NATURAL GAS SUPPLY, DEMAND, AND NODAL PRESSURES

Node	Name	Source$_i$ ($MSCF^3/hr$)		Demand$_i$ ($MSCF^3/hr$)	Electric$_i$ ($MSCF^3/hour$)		*1.a)*	*1.b)*	*1.c)*		*1.d)*	
							Press	Press	Press	Temp	Press	Temp
		1.a)/1.c)	*1.b)/1.d)*		*1.a)/1.c*	*1.b) / 1.d)*	*(PSIA)*	*(PSIA)*	*(PSIA)*	*(°R)*	*(PSIA)*	*(°R)*
1	Zeebugge	21.613	21. 6256	0.000	0.000	0.000	942.7	942.7	942.7	515	942.7	515
2	Dudzele	9.632	9.632	0.000	0.000	0.000	942.0	942.0	942.0	515	942.0	515
3	Brugge	0.000	0.000	5.7666	0.000	0.000	939.2	939.2	939.2	514.69	939.2	514.69
4	Zomergem	0.000	0.000	0.000	0.6973	0.7037	929.8	929.8	929.7	513.65	929.6	513.65
5	Loenhout	0.5620	0.5620	0.000	0.000	0.000	841.2	841.2	840.8	515	840.8	515
6	Antwerpe	0.000	0.000	5.9358	0.000	0.000	839.6	839.6	839.1	504.80	839.1	504.80
7	Gent	0.000	0.000	7.7339	0.000	0.000	845.9	845.9	845.4	504.44	845.4	504.44
8	Voeren	29.6466	29.6466	0.000	0.000	0.000	782.2	782.1	785.1	515	785.0	515
9	Berneau	0.000	0.000	0.000	0.000	0.000	942.7	942.7	942.7	515	942.7	515
10	Liege	0.000	0.000	9.3672	0.000	0.000	938.3	938.3	938.3	514.51	938.2	514.51
11	Warnand	0.000	0.000	0.000	0.000	0.000	935.2	935.1	935.0	514.16	935.0	514.16
12	Namur	0.000	0.000	3.1194	0.6094	0.6159	924.7	924.7	924.5	513.00	924.4	513.00
13	Anderlues	5.2824	5.2824	0.000	0.000	0.000	920.3	920.3	920.0	515	920.0	515
14	Peronnes	2.0703	2.0703	0.000	0.000	0.000	917.3	917.3	917.0	515	916.9	515
15	Mons	0.000	0.000	10.0764	0.000	0.000	892.4	892.3	891.6	512.23	891.6	512.23
16	Blaregnies	0.000	0.000	22.978	0.000	0.000	867.9	867.9	866.9	509.53	866.9	509.53
17	Wanze	0.000	0.000	0.000	0.000	0.000	779.7	779.6	781.0	497.33	781.0	497.33
18	Sinsin	0.000	0.000	0.000	0.000	0.000	856.2	856.2	859.0	515	859.0	515
19	Arlon	0.3016	0.3016	0.000	0.000	0.000	835.7	835.7	838.3	515	838.2	515
20	Petange	0.000	0.000	2.8237	0.000	0.000	775.7	775.6	777.9	508.39	777.8	508.39
TOTAL		69.108	69.121	6.801	1.306	1.319						

of all specified gas loads divided by the number of compressors. Based on all of these initializations, the initial values of the energy consumed by compressors and the compression ratio are computed by using (7) and (8), respectively. However, the former computation can be avoided since the gas tapped by each compressor is significantly less than the gas flowing through the network, such that a null initial value for the energy consumed by compressors is also possible.

V. CASE STUDIES

The suitability of the proposed approach for conducting steady-state flow studies of an electric power system coupled with a natural gas infrastructure is tested on two energy systems as described below.

A. Case 1

The proposed approach is applied to analyze an integrated gas-electricity infrastructure composed by the Belgian gas network [22], shown in Fig. 2, and by the IEEE-14 bus test system [23]. The 20-nodes natural gas network is composed of eight gas nonelectric loads, seven sources, 24 pipelines, and two compressors driven by an external energy source, as shown in Tables I and II. The pipelines' constants are calculated according to (2) and are given in Table I. The node referred to as Zeebugge in Table II is considered the slack node. On the other hand, the electricity infrastructure has the electric energy demand reported in Table III, and it is assumed there are two gas-fired generators at nodes 2 and 3 which are supplied from nodes 4 and 12 of the gas network, respectively. For the purpose of analysis, the gas and power flow solution was first obtained considering the gas temperature constant at 506.7 °R at all natural gas nodes and assuming the following two cases of slack nodes in the electricity infrastructure: *1.a*) a single slack node and *1.b*) distributed slack nodes. In the former, generator 2 is selected as the single slack generator to produce sufficient power for any unmet system load and for system losses, while holding all other active power generation at the set values reported in [24]. This single slack node option is simply obtained by setting $k^2_{\text{gen}} = 1$ with all other participation factors $k^i_{\text{gen}} = 0, i = 1, 3, 6$, as indicated in the second row of Table IV. In the latter, all generators regulate their active power according to the assigned participation factors reported in the third row of Table IV. A second set of flow analyses in both infrastructures is also performed considering the slack node options mentioned above but supposing a constant gas temperature of 515.0 °R only at those nodes where compressors and gas sources are connected, while for the rest of nodes the temperature is considered a state variable to be computed during the iterative solution process assuming an environmental temperature of 500 °R and a heat transfer coefficient of 0.025 BTU/ft^2 for every pipeline of the network. These cases of studies are referred to as *1.c*) and *1.d*) for the single slack node and distributed slack nodes, respectively.

The state variables were initialized according to the guidelines given in Section IV-C for all case of studies, performing two simulations for each case to consider the initialization of BHP at null values and at values computed by (7).

For each case, the same gas flow solutions were obtained independently of the BHP initialization. For cases *1.a, 1.b, 1.c, and 1.d*, the solutions were obtained in 7, 10, 7, and 10 iterations, respectively, to a mismatch tolerance of 10^{-6} in the gas network and a 10^{-12} in the electricity network. From a physical point of view and according to the proposed formulation, a tolerance of 10^{-6} in the natural gas state variables represents a nodal mismatch balance of μSCF, and in order to set a comparable framework, a tolerance of 10^{-12} in the electrical state variables corresponds to a nodal mismatch balance of 100 μVA.

The results obtained for all cases are reported in Tables I and II for natural gas flow in pipelines and natural gas nodal variables, respectively; the electric network results are shown in Table III. For purposes of validation of the proposed approach,

TABLE III
ELECTRICITY SUPPLY AND DEMAND

Node	Generation$_i$ *(MW/MVAR)* *1.a)/1.c)* P	Q	*1.b)/1.d)* P	Q	Demand$_i$ *(MW/MVAR)* P	Q
1	63.43	21.89	61.19	22.49	0	0
2	94.79	4.29	95.66	3.84	21.7	12.7
3	82.84	-6.44	83.71	-6.73	94.2	19
4	0	0	0	0	47.8	-3.9
5	0	0	0	0	7.6	1.6
6	21.64	7.84	22.07	7.76	11.2	7.5
7	0	0	0	0	0	0
8	0	17.35	0	17.35	0	0
9	0	0	0	0	29.5	16.6
10	0	0	0	0	9	5.8
11	0	0	0	0	3.5	1.8
12	0	0	0	0	6.1	1.6
13	0	0	0	0	13.5	5.8
14	0	0	0	0	14.9	5
TOTAL	262.71	44.94	262.67	44.72	259.0	73.5

the results obtained in case *1.a* are compared with the optimal equilibrium point reported in [24], both being practically the same results. Note that in the formulation proposed in [24] both networks are solved sequentially, compressors are not included explicitly in the mathematical formulation and the gas temperature is always considered constant. In the sequential solution, Newton's method is used to solve the power flow equations of the electric power system, and an interior-point linear programing approach is used to solve the gas flow problem.

Finally, the use of the chart proposed by Carroll [16] shows that, for cases *1.c* and *1.d*, three nodes (6, 7, and 17) of the gas network have a relation of nodal pressure and temperature within the unsafe operating zone with a risk of hydrate formation in the inner-wall of pipelines, as shown in Fig. 3. Based on these observations, reducing the level of pressure along the network in order to operate in the feasibility region free of hydrate formation is necessary.

B. Case 2

The analyzed energy infrastructure consists of the 54-machine, 118-bus IEEE electric power system [23] and a 15-nodes natural gas network [4]. The infrastructures are coupled via eight gas-fired generators as shown in Fig. 4. The gas network has five gas nonelectric loads, two sources, and four compressors. Two compressors are driven by gas turbines, and the gas is tapped from the inlet node of the compressor station, while the other two compressors are driven by electric motors supplied from the electric network.

The node NG-1 serves as the slack node in the gas network. The parameters of the heat rate curves are given in the Appendix, while the pipelines' and compressors' data are reported in [4]. In order to assess the temperature effect on the equilibrium point associated with the natural gas network, the following two scenarios were simulated: 1) the first scenario assumes a constant temperature of 550 °R at all natural gas nodes and considers two types of slack nodes in the electrical network, *2.a*) a single slack node as defined in the second row of Table V and *2.b*) distributed slack nodes with participation factors as reported in the third row of Table V and 2) the gas temperature is considered as a state variable to be computed

TABLE IV
PARTICIPATION FACTORS OF ELECTRIC GENERATORS

Nodes	1	2	3	6
Single slack node	0.0	1.0	0.0	0.0
Distributed slack nodes	0.5	0.2	0.2	0.1

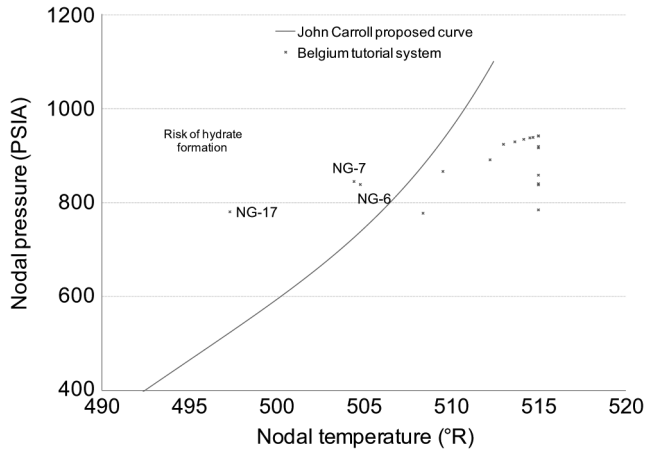

Fig. 3. Operating condition of the natural gas network for case *1.c*.

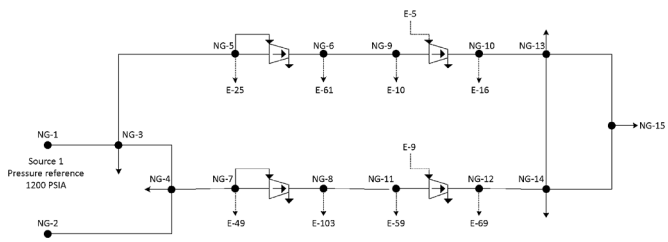

Fig. 4. The 15-node gas network coupled with the IEEE-118 network.

TABLE V
PARTICIPATION FACTORS OF ELECTRIC GENERATORS (CASE 2)

Nodes	10	16	25	49	59	61	69	103
Single slack node	0.0	0.0	0.0	0.0	0.0	0.0	1.0	0.0
Distributed slack node	0.25	0.02	0.1	0.1	0.07	0.08	0.35	0.03

during the iterative solution, except at nodes of compressors and gas sources where a constant gas temperature is set at 550 °R. In this second scenario, an environmental temperature of 500 °R and a heat transfer coefficient of 0.025 BTU/ft^2 for every pipeline of the network are assumed. Similarly to the first scenario, a single slack node and distributed slack nodes have been considered in the electricity infrastructure, as reported in Table V, to perform the steady-state analysis of the overall energy grid. These study cases are referred to as *2.c*) and *2.d*), respectively.

Power flow solutions converged in seven, six, nine, and eight iterations for scenarios *2.a*, *2.b*, *2.c*, and *2.d*, respectively, to a mismatch tolerance of 10^{-6} and of 10^{-12} for the natural gas and electricity systems, respectively.

Table VI summarizes the results for the natural gas network associated with the natural gas supply, gas demanded by gas-

TABLE VI
NATURAL GAS SUPPLY, DEMAND AND NODAL PRESSURES

Node	Source$_i$ (MSCF^3/hr)		Demand$_i$ (MSCF^3/hr)	Electric$_i$ (MSCF^3/hour)		2.a) Press	2.b) Press	2.c) Press	2.c) Temp	2.d) Press	2.d) Temp
	2.a)/2.c)	2.b)/2.d)		2.a)/2.c	2.b) / 2.d)	(PSIA)	(PSIA)	(PSIA)	(°R)	(PSIA)	(°R)
1	6.2494	6.1805	0	0	0	1200.0	1200.0	1200.0	550.0	1200.0	550.0
2	8.0000	8.0000	0	0	0	1298.3	1301.6	1294.0	550.0	1297.3	550.0
3	0	0	0.838	0	0	1034.4	1038.3	1037.8	530.6	1041.6	530.9
4	0	0	0.218	0	0	1039.6	1043.7	1042.5	522.5	1046.4	522.6
5	0	0	0	1.2556	1.2617	806.3	814.5	817.9	550.0	825.7	550.0
6	0	0	0	0.8966	0.9002	1451.3	1466.1	1472.3	550.0	1486.3	550.0
7	0	0	0	1.1537	1.1594	806.1	813.6	814.9	550.0	822.1	550.0
8	0	0	0	0.2256	0.2259	1531.6	1545.9	1548.3	550.0	1561.9	550.0
9	0	0	0	2.6938	2.7253	1372.5	1389.9	1396.5	540.0	1413.0	540.0
10	0	0	0	0.0578	0.0578	1372.5	1389.9	1396.5	540.0	1413.0	540.0
11	0	0	0	0.8675	0.8706	1275.6	1296.3	1301.0	520.0	1320.6	520.0
12	0	0	0	4.0416	3.9220	1339.3	1361.1	1366.1	520.0	1386.6	520.0
13	0	0	0.223	0	0	1342.4	1363.1	1368.7	537.0	1388.1	537.3
14	0	0	0.274	0	0	1338.8	1360.1	1365.4	531.8	1385.5	530.6
15	0	0	1.501	0	0	1335.5	1356.6	1362.2	534.4	1382.1	534.0
TOTAL	*14.2494*	*14.1805*	*3.054*	*11.1921*	*11.1233*						

TABLE VII
NATURAL GAS FLOWS AT PIPELINES AND COMPRESSORS

Pipeline	C_{km} (SCF/PSIA)	From	To	Gas flow (SCF^3/hour) 2.a	2.b)	2.c)	2.d)
1	240932.8	1	3	6.24	6.18	6.24	6.18
2	241232.7	2	4	8.00	8.00	8.00	8.00
3	289126.6	3	4	-1.27	-1.30	-1.24	-1.27
4	242008.5	3	5	6.68	6.65	6.66	6.61
5	232459.1	4	7	6.50	6.48	6.54	6.51
6	225390.3	6	9	4.53	4.48	4.50	4.45
7	141801.1	8	11	5.12	5.09	5.16	5.12
8	146427.1	10	13	1.78	1.70	1.75	1.67
9	135148.8	12	14	0.216	0.30	0.25	0.33
10	152148.7	13	14	0.640	0.58	0.62	0.56
11	158598.1	13	15	0.918	0.89	0.91	0.88
12	146339.1	14	15	0.582	0.61	0.59	0.62
Compressor		From	To	*2.a)*	*2.b)*	*2.c)*	*2.d)*
1		5	6	5.429	5.38	5.39	5.35
2		7	8	5.351	5.31	5.38	5.34
3		9	10	1.839	1.75	1.80	1.72
4		11	12	4.257	4.22	4.28	4.25

TABLE VIII
ENERGY CONSUMED BY COMPRESSORS

Compressor	From	To	Horse Power (HP) 2.a)	2.b)	2.c)	2.d)
1	5	6	184.8	183.2	183.8	182.1
2	7	8	197.8	196.6	199.0	197.8
3	9	10	0.00	0.00	0.00	0.00
4	11	12	11.16	11.06	10.63	10.54

TABLE IX
ELECTRICITY SUPPLIED BY GAS-FIRED GENERATORS

Electric	NG	Generation$_i$ (MW/MVAR) 2.a)/2.c) P	2.a)/2.c) Q	2.b)/2.d) P	2.b)/2.d) Q
10	9	450	-	454.89	-
16	10	10	18.34	10.39	18.25
25	5	220	-	221.96	-
49	7	204	8.72	205.96	7.55
59	11	155	99.66	156.37	99.36
61	6	160	-	161.57	-
69	12	645.38	-	632.25	-
103	8	40	17.04	40.59	16.84
TOTAL		1884.3	-	1883.9	-

fired plants, nodal pressures and nodal temperatures. The last two set of results are reported in order to identify the operating conditions with risk of hydrate formation according to Fig. 1. The equilibrium point obtained for each case is located within the safety zone of operation. Furthermore, these results provide information about how far the equilibrium point is from the boundary of this safety zone. By way of example, the pressure at node NG-4 has a value close to 1040 PSIA, such that the risk of hydrate formation for this value of pressure occurs for temperatures below 511 °R. As the data from columns 5 and 6 of this table show, the gas consumed by electric generators is reduced when distributed slack nodes are considered in the electrical network. However, this observation cannot be considered as a general rule because the gas consumed by fired-gas plants depends on the online regulating generators and their assigned participation factors.

The natural gas flows through pipelines and compressors as well as the energy consumption of compressors are reported in Tables VII and VIII, respectively. The former set of results numerically demonstrates that the selection of the type of the slack node in the electrical network affects the flow through the gas infrastructure, which clearly shows the interdependency between both networks. On the other hand, the results reported in Table VIII demonstrate that the energy consumed by compressors is affected by the gas temperature along the network. In these study cases, compressors consume more energy when a constant gas temperature of 550°R is assumed at all nodes of the gas network. These results are in accordance to (7), i.e., a higher gas temperature along the network, the higher the energy consumption in compression stations. Lastly, the power supplied by gas-fired generators is reported in Table IX.

TABLE X
GAS-FIRED GENERATORS' HEAT RATE CURVES

Node		Heat Rate (20)		
Electric	*Natural Gas*	α_g^i	β_g^i	γ_g^i
10	9	350000	10	2
16	10	16000	10	2
25	5	255000	10	2
49	7	240000	10	2
59	11	195000	10	2
61	6	200000	10	2
69	12	300000	10	2
103	8	60000	10	2

VI. CONCLUSIONS

This paper proposes an integrated energy flow analysis of natural gas and electric power systems. In the latter, it is assumed that an arbitrary number of gas-fired generators have variable active power as a function of gas supply to better represent the interaction between both infrastructures. Since the environmental temperature has an important impact on the design of pipelines and the operation of the natural gas network, the conventional modeling of this infrastructure has been expanded to consider the gas temperature as a state variable in order to assess the compressors' energy consumption and to identify operating conditions that could lead to harmful hydrate formation in pipelines. The set of nonlinear equations representing the combined natural gas and electricity systems have been obtained based on the nodal balance of gas and power flows, respectively. This set of equations has been linearized and solved using the Newton technique. Guidelines for the initialization of the state variables associated with the natural gas network have been proposed to circumvent the problem of an ill-conditioned Jacobian matrix if nodal pressures are initialized at the same values. Numerical examples have been presented to demonstrate the prowess of the proposed approach to analyze the interdependency between both energy infrastructures, where the generation of gas-fired plants as a function of the gas supply and the electric energy consumed by compressor motors are computed automatically together with both gas and electric state variables in a unified frame of reference.

APPENDIX

The parameters of the heat rate curves are given in Table X.

REFERENCES

[1] S. M. Kaplan, "Displacing coal with generation from existing natural gas-fired power plants," CRS Report for Congress, 7-5700, R41027, Jan. 19th, 2010 [Online]. Available: http://assets.opencrs.com/rpts

[2] M. Shahidehpour, Y. Fu, and T. Wiedman, "Impact of natural gas infrastructure on electric power systems," *Proc. IEEE*, vol. 93, no. 5, pp. 1042–1056, May 2005.

[3] A. Quelhas, E. Gil, J. D. McCalley, and S. M. Ryan, "A multiperiod generalized network flow model of the U.S. integrated energy system: Part I—Model description," *IEEE Trans. Power Syst.*, vol. 22, no. 2, pp. 829–836, May 2007.

[4] S. An, Q. Li, and T. W. Gedra, "Natural gas and electricity optimal power flow," in *Proc. IEEE PES Transm. Distrib.Conf.*, 2003, vol. 1, pp. 138–143.

[5] J. Munoz, N. Jimenez-Redondo, J. Perez-Ruiz, and J. Barquin, "Natural gas network modeling for power systems reliability studies," in *Proc. IEEE Bologna Power Tech Conf.*, 2003, vol. 4.

[6] M. Geidl and G. Andersson, "Optimal power flow of multiple energy carriers," *IEEE Trans. Power Syst.*, vol. 22, no. 1, pp. 145–155, Feb. 2007.

[7] M. Chaudry, N. Jenkins, and G. Strbac, "Multi-time period combined gas and electricity network optimisation," *Elec. Power Syst. Res.*, vol. 78, no. 7, pp. 1265–1279, Jul. 2008.

[8] C. Liu, M. Shahidehpour, Y. Fu, and Z. Li, "Security-constrained unit commitment with natural gas transmission constraints," *IEEE Trans. Power Syst.*, vol. 24, no. 3, pp. 1523–1536, Aug. 2009.

[9] F. Abdolahi, A. Mesbah, R. B. Boozarjomehry, and W. Y. Svrcek, "The effect of major parameters on simulations results of gas pipelines," *Int. J. Mech. Sci.*, vol. 49, no. 8, pp. 989–1000, Aug. 2007.

[10] S. Mokhatab, W. A. Poe, and J. G. Speight, *Handbook of Natural Gas Transmission and Processing*. Burlington, MA: Gulf Professional, Elsevier, 2006.

[11] P. M. Coeho and C. Pinho, "Considerations about equations for steady state flow in natural gas pipelines," *J. Brazil. Soc. Mech. Sci. Eng.*, vol. XXIX, no. 3/273, Jul.-Sep. 2007.

[12] R. Kehlhofer, B. Rukes, F. Hannemann, and F. Stirnimann, *Combines-Cycle Gas & Steam Turbine Power Plants*, 3rd ed. Tulsa, OK: PennWell, 2009.

[13] T. L. Coutler and M. F. Bardon, "Revised equation improves flowing gas temperature prediction," *Oil & Gas J.*, vol. 26, pp. 107–108, 1979.

[14] X. Guoyu, F. D. Galiana, and S. Low, "Decoupled economic dispatch using the participation factors load flow," *IEEE Trans. Power App. Syst.*, vol. PAS-104, no. 6, pp. 1377–1384, Jun. 1985.

[15] D. W. Shroeder, "A tutorial on pipe flow equations," Stoner Assoc. Inc., Carlisle, PA, Aug. 2001 [Online]. Available: http://www.psig.org/papers/2000/0112.pdf

[16] J. Carroll, *Natural Gas Hydrates: A Guide For Engineers*. Burlington, MA: Gulf Professional, Elsevier, 2003.

[17] J. M. Coulson, J. F. Richardson, J. R. Backhurst, and J. H. Harker, *Fluid Flow, Heat Transfer and Mass Transfer*. London, U.K.: Elsevier, 1999, vol. 1, Coulon & Richardson Chemical Engineering.

[18] E. Acha, C. R. Fuerte-Esquivel, H. Ambriz-Perez, and C. Angeles-Camacho, *FACTS: Modelling and Simulation in Power Networks*. New York: Wiley, 2004.

[19] W. F. Tinney and J. M. Walker, "Direct solutions of sparse network equations by optimally ordered triangular factorization," *Proc. IEEE*, vol. 55, no. 11, pp. 1801–1809, Nov. 1967.

[20] J. M. Ortega and W. C. Rheinboldt, *Iterative Solutions of Nonlinear Equations in Several Variables*. Philadelphia, PA: SIAM, 2000.

[21] B. Sttot, "Effective starting process for Newton-Raphson load flows," *Proc. Inst. Electr. Eng.*, vol. 118, no. 8, pp. 983–987, Aug. 1971.

[22] D. Wolf and Y. Smeers, "The gas transmission problem solved by an extension of the simplex algorithm," *Manag. Sci.*, vol. 46, no. 11, pp. 1454–1465, Nov. 2000.

[23] [Online]. Available: http://www.ee.washington.edu/research/pstca/

[24] C. Unsihuay, J. W. Marangon Lima, and A. C. Zambroni de Souza, "Modeling the integrated natural gas and electricity optimal power flow," in *Proc. IEEE PES General Meeting*, 2007, pp. 24–28.

Alberto Martínez-Mares received the B.Eng. degree (Hons) from Instituto Tecnológico de Morelia, México in 1999, and the M.Sc. degree from Universidad Autonoma de Nuevo Léon, México, in 2002. He is currently working toward the Ph.D. degree at Universidad Michoacana, Morelia, Michoacan, Mexico.

Claudio R. Fuerte-Esquivel (M'91–SM'07) received the B.Eng. degree (Hons) from Instituto Tecnológico de Morelia, México in 1990, the M.Sc. degree (*summa cum laude*) from Instituto Politécnico Nacional, México, in 1993, and the Ph.D. degree from the University of Glasgow, Glasgow, U.K., in 1997.

Currently, he is a Professor with Universidad Michoacana, Morelia, Michoacan, Mexico, where his research interests lie in the dynamic and steady-state analysis of FACTS.